Insect Systematics and Diversity, (2019) 3(4): 3; 1–12
doi: 10.1093/isd/ixz013
Research article

Molecular phylogenetics, phylogenomics, and phylogeography

A Phylogenetic Analysis of the Dirt Ants, *Basiceros* (Formicidae: Myrmicinae): Inferring Life Histories Through Morphological Convergence

Rodolfo S. Probst,[1,6] Brian D. Wray,[2] Corrie S. Moreau,[3,4] and Carlos R.F. Brandão[5]

[1]School of Biological Sciences, University of Utah, 257 S 1400 E, Salt Lake City, UT 84102, [2]Center for Genetic Medicine, Feinberg School of Medicine, Northwestern University, 420 East Superior Street, Chicago, IL 60611, [3]Department of Entomology, Cornell University, 129 Garden Avenue, Ithaca, NY 14853, [4]Department of Ecology and Evolutionary Biology, Cornell University, 129 Garden Avenue, Ithaca, NY 14853, [5]Laboratório de Hymenoptera, Museu de Zoologia da Universidade de São Paulo, Avenida Nazaré, 481, São Paulo, SP 04263-000, Brazil, and [6]Corresponding author, e-mail: probstrodolfo@gmail.com

Subject Editor: Eduardo Almeida

Received 18 April, 2019; Editorial decision 7 July 2019

Abstract

Ants of the genus *Basiceros* Schulz, 1906 are elusive species known only from Neotropical rainforests. Little information is available regarding their natural history, and nothing is known about the phylogenetic relationships among species within the genus. The genus has been the subject of some controversy regarding generic delimitation but is currently a member of the '*Basiceros*-genus group' following recent classification changes. For mouthparts, labral and mandibular morphologies present considerable variation in the *Basiceros*-genus group, likely a result of adaptive evolution. In *Basiceros*, those differences can be observed in the labrum shape and the various degrees of development of the labral cleft and the clypeomandibular space. Here, in an attempt to illuminate the evolution of the group, species boundaries are tested for *Basiceros*. The evolutionary relationships of its species are investigated using molecular and morphological data. Bayesian inference and maximum likelihood analyses of a molecular dataset consisting of up to nine genes (three mitochondrial, six nuclear) and including samples from multiple populations of all known *Basiceros* taxa recovered the monophyly of the genus and of its species, with two well-resolved internal clades: the *singularis* clade and the *disciger* clade. Focusing on the female castes of *Basiceros*, an ancestral state reconstruction is presented for mandibles and labrum morphology. The results suggest that the labrum and clypeomandibular morphologies are highly labile, although phylogenetically important characters in the genus. Mouthpart traits indicate a strong correlated evolutionary history potentially associated with specialized feeding habits.

Key words: Attini, labrum, mandible, morphological evolution, convergence

The Neotropical genus *Basiceros* Schulz, 1906 is a small group of cryptobiotic ants distributed across the rainforests of South and Central America, from Honduras to Southern Brazil, with eight described species (Bolton 2019). Little is known about the biology of *Basiceros*, and most collections are of stray workers or colony fractions captured in passive traps. These ants apparently have relatively small-sized colonies and are known to move slowly (Wilson and Hölldobler 1986), which could explain the infrequency of whole-colony collections. Additionally, the elusiveness of *Basiceros* is reinforced by an impressive form of crypsis exhibited by adult workers and queens, which accumulate soil and leaf litter particles on their integument with the aid of specialized setae (Hölldobler and Wilson 1986; Fig. 1A).

Basiceros belongs to a clade along with five other genera: *Eurhopalothrix* Brown & Kempf, 1961; *Octostruma* Forel 1912; *Protalaridris* Brown, 1980; *Rhopalothrix* Mayr, 1870; and *Talaridris* Weber, 1941. Until recently, the clade was classified as the Basicerotini, a tribe delineated by Brown (1949). A recent molecular study (Ward et al. 2015) presented a revised tribal-level classification of the Myrmicinae, placing the clade in an expanded tribe Attini, and referring to the former Basicerotini as the informal '*Basiceros* genus-group'.

Using morphological data, Baroni Urbani and De Andrade (2007) presented the first phylogenetic hypothesis for the *Basiceros*-genus group, and in the absence of convincing synapomorphies, synonymized all of the genera under the single genus *Basiceros*. This classification faced some opposition after publication, and part of the myrmecological community has continued using the classification in Bolton (2003; also see Bolton 2019). Unpublished molecular data (M. G. Branstetter et al., in preparation), including wide taxon

sampling throughout the *Basiceros*-genus group, recover a monophyletic *Basiceros* in the narrow sense of Bolton (2019), also the definition used in this study. In short, *Basiceros* can be diagnosed as an assemblage of relatively medium-sized ants, sharing a densely sculptured integument covered with specialized pilosity, 12-segmented antennae, and a broadly flattened antennal scape with a conspicuous basal lobe.

Generic boundaries within the *Basiceros* genus-group have traditionally been based on head characters, primarily on the number of antennal segments and characteristics of the mouthparts (Brown 1949, 1974; Brown and Kempf 1960; Bolton 2003). In *Basiceros*, all species have 12-segmented antennae, a unique though presumably plesiomorphic feature in the genus group. The shapes of the mandibles and labrum vary greatly among genera and species of the genus group (Fig. 1B). In the case of *Basiceros*, with fewer than a dozen species, the mandibles and labrum show striking variation. This variation presumably plays a role in hunting behavior (Wilson and Brown 1984).

It is well documented that similar mandibular and labral shapes have convergently evolved multiple times in distantly related ant lineages (Gotwald 1969, Hölldobler and Wilson 1990, Larabee and Suarez 2014). However, few studies have examined the evolution of ant mandibular or labral characters under a rigorous phylogenetic reconstruction (Janda et al. 2004, Keller 2011, Larabee et al. 2016). Considering the variation of mandible and labrum morphology in the *Basiceros*-genus group, a species-level phylogeny would be a valuable tool for a first step investigating the lability of those traits for that clade and potentially linking morphological evolution with feeding ecology. To account for that, for this study, molecular and morphological data are used to investigate phylogenetic relationships and mouthpart evolution in *Basiceros*. We test species boundaries with molecular data of multiple individuals for most species and reconstruct a species-level phylogeny for the genus as a whole. Based on the inferred topology, the evolution of the labrum and mandibles is investigated for the female castes of all known species.

Materials and Methods

Taxon Sampling

As part of a taxonomic revision for the genus (R.S.P. and C.R.F.B., in preparation), specimens of all *Basiceros* species plus selected outgroups were examined from multiple collections (Supp File S1 [online only]) and AntWeb (https://www.antweb.org), an online specimen database with high-resolution images. Fifteen taxa were analyzed: nine *Basiceros* species (eight valid and one undescribed taxon) and five outgroups, selected based on previous studies on

Fig. 1. (A) *Basiceros manni* (Brown and Kempf 1960) adult workers from the same colony, showing age-related accumulation of integumental camouflage (photograph by Rodolfo Probst). (B) Examples of mouthpart diversity found in the *Basiceros*-genus group; from left to right: *Talaridris mandibularis* (Brazil, CASENT0235384. Image from www.antweb.org, by Estella Ortega), *Eurhopalothrix gravis* (Mann 1922) (Costa Rica, INBIOCRI001237722. Image from www.antweb.org, by Brendon Boudinot), *Rhopalothrix stannardi* Brown & Kempf, 1960 (Belize, CASENT0280781. Image from www.antweb.org, by Estella Ortega), *Basiceros scambognathus* (Brown 1949) (Brazil, scale bar: 0.5 mm). (C) An adult worker of *Basiceros singularis* preying on gastropod (Mollusca: Gastropoda), Ecuador: Tiputini. Photograph by Mark W. Moffett/Minden Pictures, all rights reserved, the permission of the author for reproduction in the present study.

the phylogeny of Formicidae which included representatives from the *Basiceros*-genus group: Dietz (2004) and Baroni Urbani and De Andrade (2007) for morphological data and Moreau et al. (2006), Brady et al. (2006), and Ward et al. (2015) for molecular data. Species and morphospecies for the outgroups were as follows: *Octostruma iheringi* (Emery 1888), *Octostruma petiolata* (Mayr 1887), *Octostruma rugifera* (Mayr 1887), *Octostruma aff. rugifera*, and *Eurhopalothrix gravis* (Mann 1922). The latter was selected as the rooting point given the phylogenetic position of this genus in the *Basiceros*-genus group (sensu Ward et al. 2015). *Basiceros* specimens were included taking into account the distributional range when possible, totaling 40 *Basiceros* specimens (Supp Table S1 [online only]). *Basiceros redux* (Donisthorpe 1939), a species described from a single male, is excluded from the study because we were not able to obtain recently collected specimens. Male morphology in *Basiceros* is now sufficiently known to exclude *B. redux*, and it will be transferred to a different genus as a product of the taxonomic revision of the genus (R.S.P. and C.R.F.B., in preparation).

DNA Extraction and Sequencing

Specimens used for DNA analyses either came from collections made by the authors or sorted from different ethanol collections, then transferred to vials containing 96% ethanol and kept at −4°C until extraction. Museum material (pinned specimens) collected between 1992 and 2015 was also included by unmounting specimens before extraction. For singletons and pinned material, a nondestructive protocol provided by P. Ward (University of Davis, CA, personal communication) was followed, adapting it as needed based on the samples available. For all other specimens, DNA was extracted destructively (from the entire specimen or the three right legs) and vouchers belong to the same series. All laboratory work was performed according to the protocols in Moreau (2014). The material used for destructive extraction was ground with metal beads on a TissueLyser (Qiagen, Inc., Valencia, CA) for 30 s before starting the extraction. All extractions were performed using the Qiagen DNeasy Blood and Tissue Kit (Qiagen, Inc.). Supp Tables S1 and S2 (online only) contain information for all voucher specimens.

We attempted to amplify nine gene fragments from each sample using traditional polymerase chain reaction (PCR) and Sanger sequencing methods. The following gene fragments were used: three mitochondrial genes (*cytochrome oxidase subunit 1* [CO1], *cytochrome B* [CytB], and *ribosomal 12S rDNA* [12S]) and six nuclear protein-coding genes (*arginine kinase* [*ArgK*], *elongation factor 1 alpha F1* [*EF1aF1*], *elongation factor 1 alpha F2* [*EF1aF2*], *long-wavelength rhodopsin* [*LWRh*], *RNA polymerase II* [*RNA_pol-II*], and *Wingless* [*Wg*]). Region-specific primers for each gene were obtained from different sources (Supp Table S3 [online only]) and ordered from Integrated DNA Technologies (IDT; Coralville, IA).

Double-stranded DNA was amplified in 25-µl volume reactions: 2.0 µl of extracted gDNA, 14.4 µl of ultrapure water, 1.2 µl of each of the two primers (10 mM), 2.5 µl of buffer (Tris 10× at pH 8.0, with $MgCl_2$ included), 2.5 µl of dNTPs (0.8 mmol), 1.0 µl of bovine serum albumin (BSA), and 0.2 µl of Taq DNAPolymerase (Roche, Indianapolis, IN). Samples that did not amplify after the first or second try were further attempted using PCR beads (Illustra PuReTaq Ready-To-Go; GE Healthcare, Chalfont St. Giles, United Kingdom). For the PCR bead reactions, 1.0 µl of the forward and the reverse primers (10 mM) and 23 µl of ultrapure water were added to each bead, for a total reaction volume of 25 µl; that mixed reaction being split in half for two reactions per bead, to which 0.5 µl of gDNA was added. All the reactions were subjected to the following thermal cycler parameters: 1-min initial denaturation at 94°C; followed by 30 cycles with 1-min denaturation at 94°C, annealing temperature 45–54°C for 1 min depending on the fragment being amplified, extension temperature 72°C for 2 min, and a final extension at 72°C for 3 min. The amplified DNA products were then visualized by agarose gel electrophoresis with ethidium bromide (2%). Successful PCR products were cleaned using 2 µl of ExoSAP-IT (General Electric, Piscataway, NJ) following the manufacturer's protocol for the 23 µl (post-gel) PCR product volume: the reaction was run in a thermocycler with 37°C for 15 min and 80°C for 15 min. The same primers used for cycle sequencing reactions were used for PCR amplification. All PCR products were sequenced in both directions. For these reactions, a volume of 10.0 µl was used.

The cleaned PCR products were used as a template for cycle sequencing reactions using Big Dye Terminator 3.1. These reactions were cleaned by EtOH/EDTA precipitation (following Moreau 2014). Amplifications were then resuspended and sequenced from complementary strands using the DNA sequencer ABI 3730 DNA Analyzer (Applied Biosystems, Waltham, MA). The chromatograms were edited and compiled using the program Geneious 6.1.6 (Biomatters Limited, AK, New Zealand). Consensus sequences were quality-checked using BLAST (Basic Local Alignment Search Tool) from the NCBI platform (National Center for Biotechnology Information), available at http://blast.ncbi.nlm.nih.gov/Blast.cgi.

For the species *Basiceros convexiceps* (Mayr 1887), a suitable sequence could not be obtained using the PCR methods outlined above. To include *B. convexiceps* and to improve the completeness of the molecular matrix for other species, candidate sequences were mined from Illumina next-generation sequencing data generated for a phylogenomic study (M. G. Branstetter et al., unpublished data). The sequences were generated following the ultraconserved element (UCE) phylogenomic approach described in Branstetter et al. (2017), which involves the targeted enrichment of UCE loci and a set of traditional Sanger sequencing genes, including most of the ones used here (*ArgK*, *EF1aF1*, *EF1aF2*, *LWRh*, *CO1*). All successfully amplified and sequenced eight fragments have been deposited in GenBank (see Supp Table S2 [online only] for accession numbers). The sequences obtained for the 12S gene are included as Supp File S2 (online only) in the FASTA format, as sequences available on GenBank were too few to allow a safe annotation for the 12S sequences generated for this study.

Sequence Alignment

A first alignment for the sequences was performed with the program Geneious 6.1.6 using the ClustalW alignment option (Larkin et al. 2007). A further step of alignment was done with the program MAFFT 7 using the iterative refinement method (Katoh and Standley 2014). Subsequently, the sequences were visualized and aligned by eye for further adjustments with the program MEGA 7.0.21 (Kumar et al. 2015). The final alignments were quality-checked by translating the sequences into amino acids and checking the reading frames. Regions corresponding to the primer sequences were deleted. The sequences were then 'trimmed' to a shared length and questions marks (?) were replaced by gaps (-) at the ends of sequences. The most inclusive alignment comprised 4,334 bp (including gaps and missing data, excluding introns) for 46 specimens, with each specimen having up to nine genes (Supp Table S2 [online only]). It is important to mention that due to the rarity of material in good conditions for DNA extractions, our molecular matrix experiences a considerable degree of incompleteness (see Supp Table S2 [online only]), both in what we are calling the full and pruned1 and pruned2

datasets (see Phylogenetic Analyses). In our complete dataset (n = 46 specimens), the mean number of sequenced loci was 4 (range from 1 to 9). For the pruned1 and pruned2 datasets (n = 36 and n = 13, respectively), the mean number was close to 5 (range from 2 to 9 and range from 1 to 9, respectively; see Supp Table S4 [online only] for summary of matrices' characteristics). Matrices and partition files are available from Dryad (doi:10.5061/dryad.bd4ch22).

Phylogenetic Analyses

Three datasets were analyzed to determine monophyly and relationships among *Basiceros* species for all the taxa included in the study: 'full', 'pruned1', and 'pruned2'. The full dataset included all specimens. Additionally, to account for the effect of incompleteness, an additional Bayesian inference (BI) and maximum likelihood (ML) analyses with 36 specimens (pruned1 dataset) were conducted, excluding those terminals from which only one genetic fragment was sequenced. The pruned2 dataset included one specimen per species and the selection of terminals was based on the specimens for each species having the most data (matrix completeness was favored when the number of sequenced loci was equal).

The full dataset (46-taxon, 9-gene matrix) was initially partitioned into 25 blocks, corresponding to the codon positions of each of the eight protein-coding genes and one block for *12S rDNA*. Models of nucleotide substitution were selected running each partition in the program jModelTest 2 (Darriba et al. 2012) and comparing best scores for both corrected Akaike's information criteria and Bayesian information criteria, yielding an 11-partition scheme (Supp Table S5 [online only]), which was used in subsequent BI and ML analyses. All phylogenetic analyses for this study were performed on the CIPRES Science Gateway, version 3.3 (Miller et al. 2010; http://www.phylo.org/), using MrBayes 3.2.5 (Ronquist et al. 2012) for BI analyses and GARLI 0.951 (Zwickl 2006) for ML analyses. Trees were visualized and edited using FigTree 1.4.3 (Rambaut 2016). For the BI analyses, all parameters were kept unlinked across the partitions except branch lengths and topology. A Markov chain Monte Carlo of 25 million generations was run, with nchains = 4, nruns = 2, sample freq = 1,000, and the default 25% burn-in. A majority-rule consensus tree was obtained with contype = halfcompat. Convergence of runs was ensured by only accepting analyses where the average standard deviation of split frequencies was below 0.001 in the post-burn-in samples and assessed in TRACER v1.7.1 (Rambaut et al. 2018). For the ML analyses, the same partitions as in MrBayes were used, and the following modifications from GARLI defaults: topoweight = 0.01, brlenweight = 0.002, modweight = 0.0065, and genthreshfortopoterm = 2,000,000. We carried out one round of eight search replicates in estimating the ML tree. Separately we ran two independent bootstrap analyses with 100 replicates (one search replicate per bootstrap replicate) and the same settings as the ML search except that genthreshfortopoterm = 1,000,000. Visualization of bootstrap values were made on the ML tree with best score by using the program SumTrees 4.0.0 (Sukumaran and Holder 2015), distributed and installed as part of DendroPy 4.0.0 (Sukumaran and Holder 2010). Parameters for the analyses with the full and pruned datasets were the same.

Ancestral Trait Reconstruction of Mouthpart Characters

To evaluate morphological evolution in *Basiceros*, ancestral character reconstructions were conducted for the labrum (general shape and distal margin; Figs. 2 and 3) and clypeomandibular space (i.e., with the mandibles closed, the presence of a gap between the anteroclypeal margin and the basal margin of the mandibles; Fig. 4) of the female castes of all taxa. Multiple individuals for each taxon (when possible) were examined to help define morphological states.

To examine mouth morphology, a Leica MZ9[5] or a Leica EZ4 stereomicroscope was used. Specimens were immobilized with ethanol-immersed Blu-Tack (Bostik, Indianapolis, IN). Labra were removed from the heads by inserting a size 1 entomology pin in the clypeolabral suture. Labra were slide-mounted dorsal face up in a drop of K-Y lube on the center of the slide and covered with a cover glass. Stacked photomicrographs of the slides were generated using Leica Application Suite V3.7 from source images captured using a Leica Z16 APO stereomicroscope coupled with a Leica DCF450 camera. All images were edited in Adobe Photoshop CS6 (Adobe Systems Inc., San Jose, CA). Vouchers of labra are located in the RSP Personal Collection.

For the general shape of labrum, the examination of *Basiceros* specimens revealed the following states: 1) long triangular and sinuate, where the sides of the labrum are concave toward the distal margin (Fig. 2A, C, and D), 2) long triangular and acute, where the sides of labrum are linearly narrowed toward the distal margin (Fig. 2B and H), 3) triangular short (hereafter short), with a wide basal portion (Fig. 2E), and 4) lunate, with a D-shaped aspect (Fig. 2F and G). For the distal margin of labrum, the states were as follows: 1) lobes with wide cleft (Fig. 2C), 2) lobes with narrow cleft (Fig. 2A, B, D, and H), 3) blunt lobes with short cleft (Fig. 2E), and 4) rounded (Fig. 2F and G). In the case of the clypeomandibular space, for *Basiceros* species, this character is either 1) absent (Fig. 4B–D), 2) narrow (Fig. 4A), 3) moderate (Fig. 4H), or 4) broad (Fig. 4E–G). Character states were mapped onto an ultrametric tree, obtained submitting the output phylogram of the BI analysis with the pruned1 dataset to the *chronos* function of the APE R package (Paradis et al. 2004), while keeping the same topological structure by maintaining only one terminal per species. Maximum likelihood reconstructions were generated using the *ace* function of the APE R package (Paradis et al. 2004). All characters states were treated as discrete, comparing equal rates (ER), symmetrical rates (SYM), and all rates different (ARD) models. The likelihood of pairwise comparisons between nested models was accessed using a likelihood ratio test (ANOVA).

Results

Phylogeny

All phylogenetic analyses (BI, ML) recovered *Basiceros* as monophyletic with high support values (Bayesian posterior probability [PP] 0.96–1.0, maximum likelihood bootstrap support [MLBS] 98–100%; Fig. 5, Supp Fig. S1 [online only]). Results for the full and pruned datasets are discussed below.

Full Dataset Analyses

For the full dataset, outputs of both analyses were mostly congruent, recovering all *Basiceros* species as monophyletic and delimiting two major clades within the genus: '*singularis*' and '*disciger*' (Supp Fig. S1A and B [online only]). The *singularis* clade (PP 0.96, MLBS 56%) has *Basiceros* sp. n. A sister to *B. convexiceps* (PP 0.87, MLBS 32%) and that clade sister to *Basiceros manni* Brown & Kempf, 1960 + *Basiceros singularis* (Smith, F., 1858). For the *disciger* clade (PP 0.96, MLBS 96%), both analyses recovered *Basiceros scambognathus* (Brown 1949) as sister to the remaining species in that clade, with *Basiceros conjugans* Brown, 1974 sister to a clade of *Basiceros disciger* (Mayr 1887) and *Basiceros militaris* (Weber 1950).

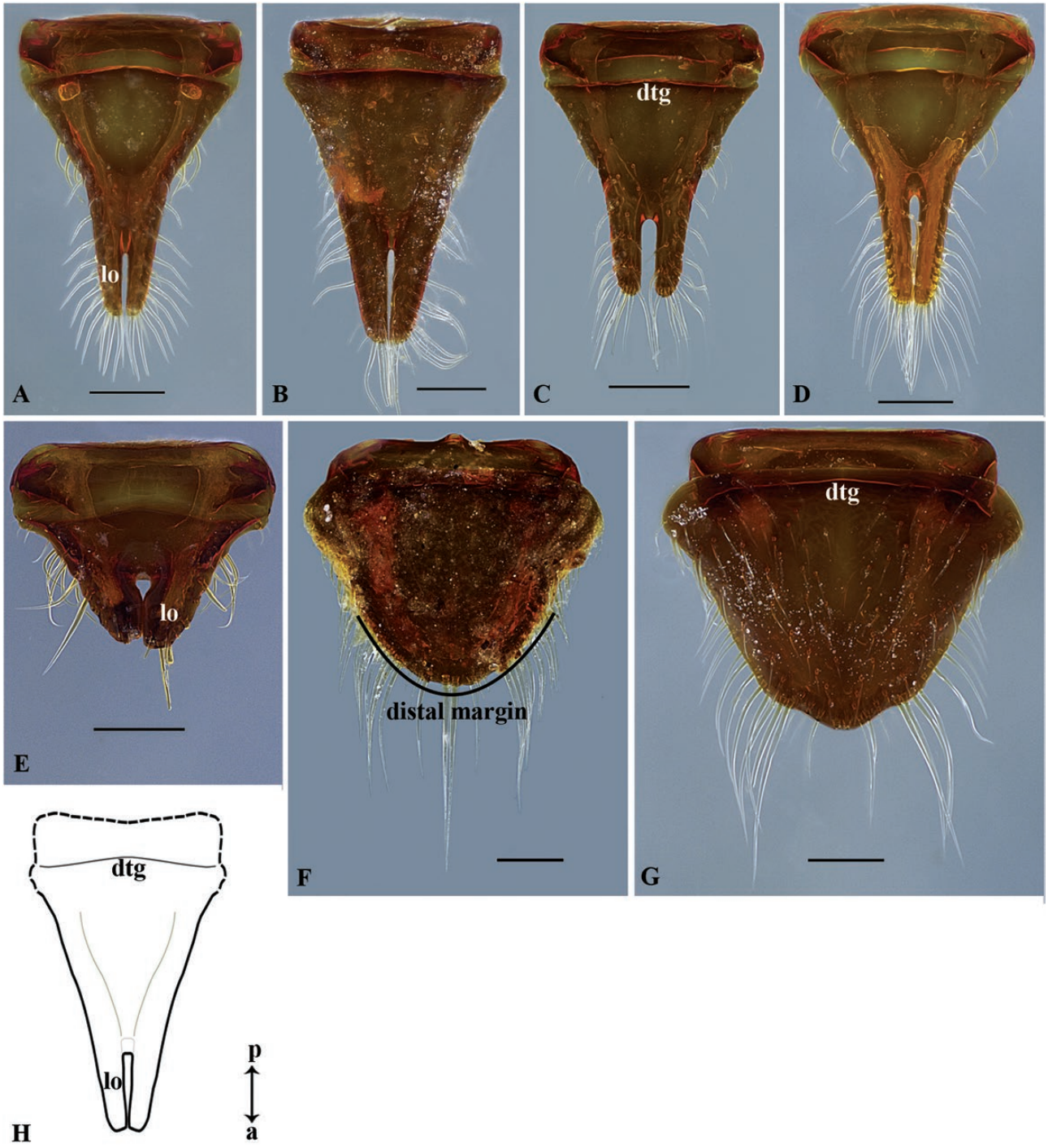

Fig. 2. Dorsal view of the labrum (dorsolabrum) of the worker caste of *Basiceros* species, dtg: dorsal transverse groove, lo: lateral lobe. (A) *B. conjugans*; (B) *B. convexiceps*; (C) *B. disciger*; (D) *B. militaris*; (E) *B. scambognathus*; (F) *B. singularis* (CASENT063735); (G) *B. manni*; (H) *Basiceros* sp. n. A, dashed line: tentative reconstruction of posterolabral limits. Crossed arrows give the orientation: a, anterior; p, posterior. Scale bar: 0.1 mm. Labrum shape in *Basiceros* can be long triangular and sinuate (A, C, D), long triangular and acute (B, H), triangular short (E) or (F, G) lunate. For the distal margin of labrum lobes can have a wide (C) or narrow clef (A, B, D, H), can be blunt with a short cleft (E) or rounded (F, G).

Pruned1 Dataset Analyses

The analyses containing 36 terminals recovered the same topology for species relationships observed at the full dataset, most species-level relationships maximum supported. The *disciger* clade was recovered with high support (PP 1.0, MLBS 99%), although only the BI analysis recovered a highly supported *singularis* clade (PP 1.0, MLBS 65%). BI analysis recovered maximum supported species relationships within the *disciger* clade, which was not observed for the position of nodes involving *B. conjugans*, *B. disciger*, and *B. militaris* for the ML analysis (MLBS 85%).

Pruned2 Dataset Analyses

The BI and ML recovered the *singularis* and *disciger* clade (Supp Fig. S1C and D [online only]). In the *singularis* clade, ML analysis

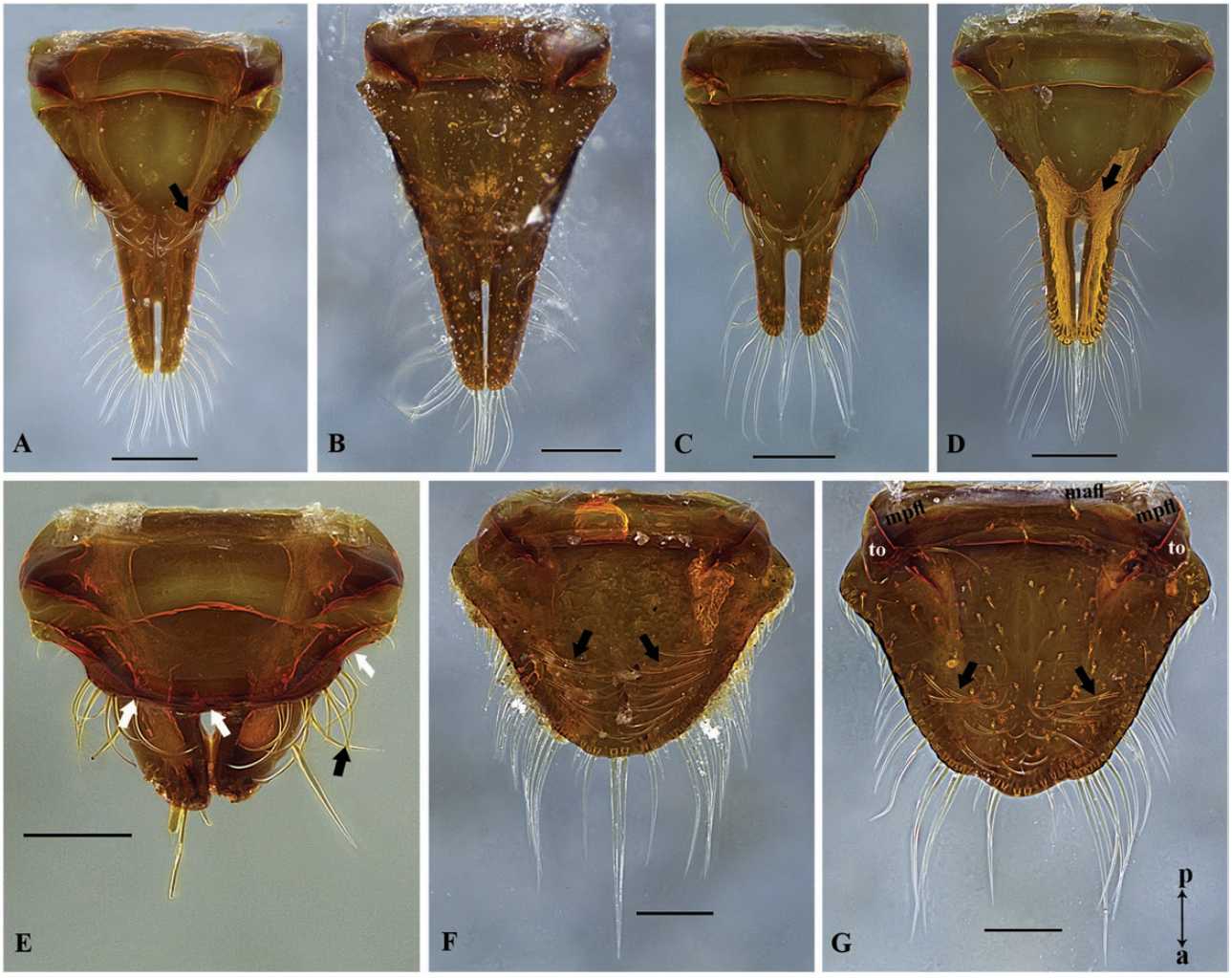

Fig. 3. Ventral view of the labrum (ventrolabrum) of the female caste of *Basiceros* species, black arrows: an example of specialized ventral setae. (A) *B. conjugans*; (B) *B. convexiceps*; (C) *B. disciger*; (D) *B. militaris*; (E) *B. scambognathus*; white arrows point to the anterior margin of the 'basal plate'; (F) *B. singularis* (CASENT063735); (G) *B. manni*, mpfl: posterior frontolabral muscle remnants, mafl: anterior frontolabral muscle remnants, to: torma. Crossed arrows give the orientation: a, anterior; p, posterior. Scale bar: 0.1 mm.

recovered low supported relationships, with *B. convexiceps* as sister to the remaining species on that clade (MLBS 60%), and *Basiceros* n. sp. A sister to *B. manni* + *B. singularis* (MLBS 55%). In the topology obtained with the BI analysis, the placement of *B. convexiceps* is not resolved. Both analyses recovered *B. manni* sister to *B. singularis* with maximum support. In the maximum supported *disciger* clade, both analyses recovered *B. scambognathus* as sister to the remaining species in that clade. However, the ML analysis recovered *B. disciger* sister to a poorly supported clade comprising *B. conjugans* and *B. militaris* (MLBS 45%), whereas the BI analysis infers *B. conjugans* as sister to a moderately supported (PP 0.75) clade of *B. disciger* and *B. militaris*.

Ancestral State Reconstruction for Morphological Characters

For all morphological traits, the ER was the favored model (Fig. 6; Supp Figs. S2 and S3 [online only]), as determined by likelihood ratio tests. Additionally, the standard errors for both SYM and ARD models were larger or sometimes represented by NaNs, suggesting a nearly flat likelihood surface, thus undermining the reconstructed rates for those models. More detailed information for the outcomes from all three models can be found in Supp Table S6 (online only).

The ER model recovered a long triangular and sinuate labrum as the most likely ancestral condition for the general labrum shape of the whole genus *Basiceros* (empirical Bayesian posterior probability [EPP] 0.405), followed by a long triangular and acute labrum (EPP 0.267). The ancestral condition for the *singularis* clade was a long triangular and acute labrum (EPP 0.375), although the model also recovered a sinuate labrum with a similar support value (EPP 0.316). Internally to this clade, the model also favored the long triangular and acute labrum for the node of *Basiceros* sp. n. A and *B. convexiceps* (EPP 0.526), and a lunate labrum for the species *B. singularis* and *B. manni* (EPP 0.698). For the *disciger* clade, the most likely ancestral condition was a long triangular and sinuate labrum (EPP 0.657), condition also recovered internally for all nodes of that clade (EPP 0.848–0.897).

Regarding the distal margin of the labrum, the model recovered the bilobed labrum with a narrow cleft as the most likely ancestral state for the whole genus (EPP 0.715) and most nodes inside *Basiceros* (0.714–0.778). The model recovered a labrum with a rounded distal margin as the most likely ancestral state for the

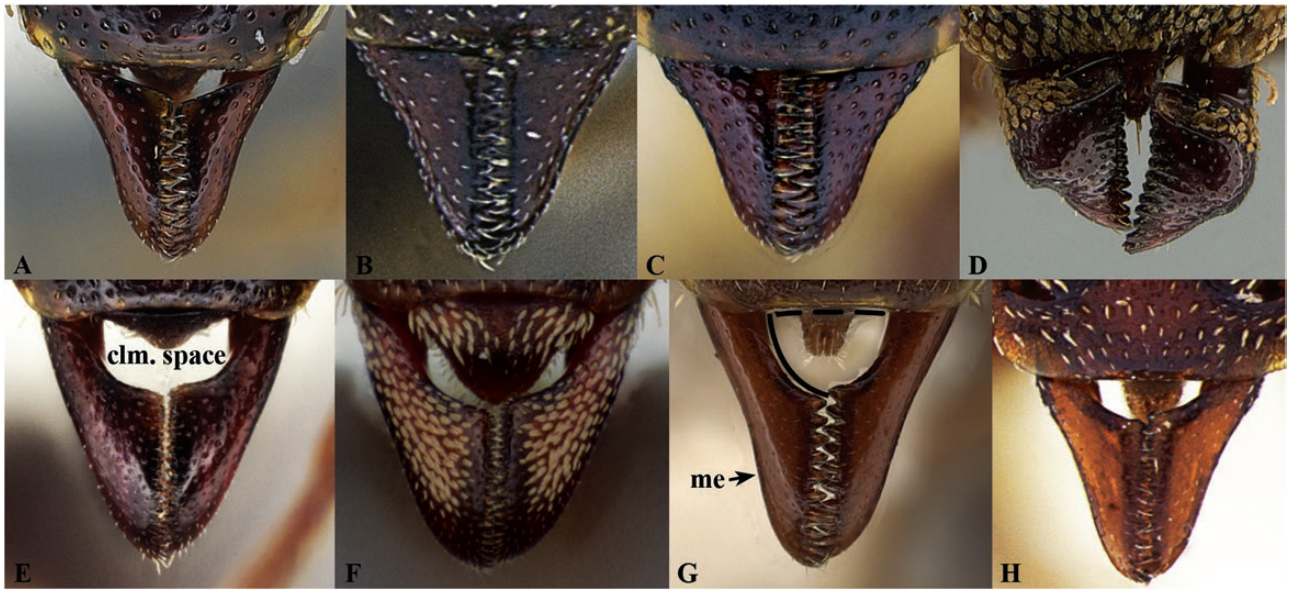

Fig. 4. Frontal view of *Basiceros* species, highlighting mandible shape and clypeomandibular space of the female caste. (A) *B. conjugans*; (B) *B. disciger*; (C) *B. militaris*; (D) *B. scambognathus*; (E) *B. manni*, clm. space: clypeomandibular space; (F) *B. singularis*; (G) *Basiceros* sp. n. A, me: external margin, dashed line: anteroclypeal margin, bold line: basal margin; (H) *B. convexiceps*. Figures not to scale. In *Basiceros*, the clypeomandibular space is either absent (B–D), narrow (A), moderate (H), or broad (E–G).

node containing *B. singularis* and *B. manni* (EBB 0.622). The same model also inferred a broad clypeomandibular space as the ancestral condition for the whole genus (EPP 0.451), followed by the absence of a clypeomandibular space (EPP 0.409). For the *singularis* clade, the ancestral condition favored was a broad clypeomandibular space (0.687). Internally to this clade, a broad clypeomandibular space was the most likely ancestral condition (EPP 0.946–0.981). In all nodes of the *disciger* clade, the model favored the ancestral condition for the clypeomandibular space as being absent (EPP 0.739–0.859).

Discussion

Phylogeny

Under the scope of our work, *Basiceros* is confirmed as a monophyletic group with strong support, supporting Bolton's (2019) classification. Both BI and ML analyses recovered very similar topologies for analyses with the full and pruned datasets (Fig. 5, Supp Fig. 1 [online only]).

The topologies obtained with the full and pruned2 datasets suggest, respectively, an effect of missing data and the importance of comprehensive population sampling for phylogenetic analysis when dealing with species boundaries. Although mostly congruent, topologies obtained for the pruned1 and full dataset recovered most relationships for the latter with fairly lower support values, the exception being the slightly better-supported clade of *B. convexiceps* as sister to *Basiceros* sp. n. A (PP 0.87/MLBS 45% vs 0.83/32%, respectively). In contrast, the BI analysis with the pruned2 dataset recovered *B. convexiceps* as a polytomy inside the *singularis* clade, and low support for the relationship between *B. militaris* and *B. disciger*. Although those node conflicts were not present for the ML analysis with the pruned2 dataset, the topology recovered did not provide strong support for relationships within the *singularis* clade. Considering these conflicts, the topology obtained with the pruned1 dataset seems to better reflect the evolutionary history for the group and henceforth is the one used for the phylogenetic discussion.

The recovered relationships within the *singularis* clade suggest an ambiguous scenario for the evolution of *Basiceros* when taking into account the biogeography of its species and support values for some of the nodes (see Fig. 5). Considering the topology obtained for the whole genus and the observed similarities within representatives of the *singularis* clade, one could speculate that the genus *Basiceros* might have originated either in the Brazilian Atlantic Forest or in the northwestern portion of the Amazon biome (see Fig. 7). Brown and Kempf (1960) considered the Atlantic Forest endemic *B. convexiceps* to be the species with the most generalized morphology belonging to the more inclusive *Basiceros*-genus group. According to them, the radiation of that group probably started in an ancestral stock similar to *B. convexiceps* when considering the morphology of the labrum (see labrum discussion below), head shape, and pilosity. For the *singularis* clade, the sister taxon to *B. convexiceps* is *Basiceros* sp. n. A, only known from a couple of collections made in the Ecuadorian Amazon (Fig. 7A).

For the *disciger* clade, the distribution of its species could indicate different degrees of past biogeographic connection between the Atlantic Forest and the Amazon (Fig. 7B). Both *B. scambognathus* and *B. conjugans* have a somewhat northern South American distribution. *Basiceros conjugans* seems to be an Amazon endemic, and its range is restricted to the northern part of that biome, a similar geographic pattern observed for *B. militaris*. The most widespread taxon within the genus is *B. disciger*, that species having a 'V-shaped' circum-Amazonian distribution, with records for the whole range of the Atlantic Forest, the Bolivian-Paraguayan Chacoan region and scattered records in the east side of South America across the seasonally dry forests reaching Venezuela (Fig. 7B). *Basiceros disciger* and *B. militaris* show very similar male and female morphologies. The worker caste of those two taxa are diagnosed by a vertexal crest present in both species, complete in *B. militaris* and emarginated medially in *B. disciger*. Interestingly, that character has considered diagnostic for supporting the description of *Aspididris*, latter synonymized under *Basiceros*. The sister species to that clade was *B. conjugans*, relationship justified when considering the overall similarity observed for males and females of those three species.

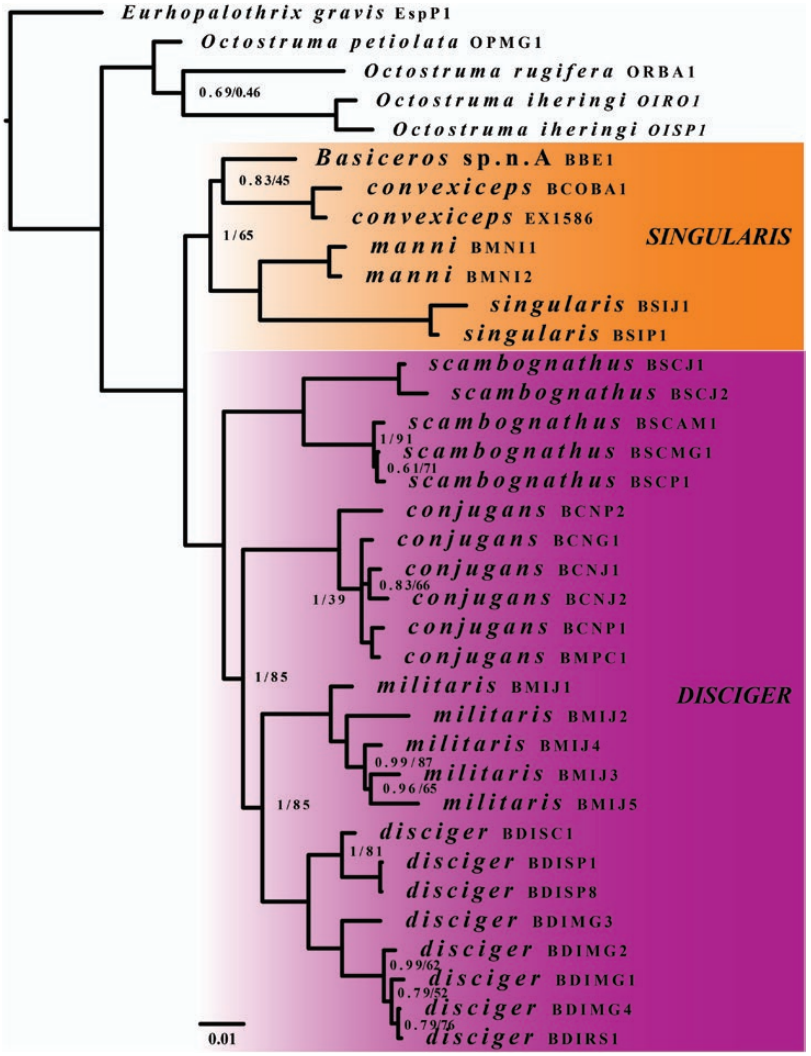

Fig. 5. Phylogeny of *Basiceros* ants, analysis with the pruned1 dataset. See Supp Tables S1 and S2 (online only) for taxon codes and further specimen information. Topology presented was obtained from MrBayes and GARLI analyses. Branch length follows MrBayes output, scale bar indicates estimated number of nucleotide substitutions per site. Bayesian posterior probability (PP, obtained with MrBayes) or maximum likelihood bootstrap support (MLBS, obtained with GARLI) values are indicated in most nodes, except for those recovered with high support (>0.95/95%) for both analyses.

However, all of those relationships within the *disciger* clade were not maximum supported, although this may be a result of the incompleteness of our molecular dataset.

The placement of the bizarre *B. scambognathus* inside *Basiceros* reinforces Feitosa et al. (2007) combination of *Creightonidris scambognatha* within *Basiceros*. Brown (1949) described the genus *Creightonidris* to accommodate *B. scambognathus*, a species morphologically unique in its mandibular shape (see Fig. 4D for detail of aberrant mandibles, with a deep transverse–oblique groove in the base of the mandibular surface) and squamiform head pilosity (see Fig. 1B). Still, virtually nothing is known about the natural history of this species. Interestingly, the recovered topology for the complete dataset in both BI and ML analyses infer two sister clades for the included *B. scambognathus* specimens. One clade grouped three specimens, all males, from Amazonas State (North of Brazil), Minas Gerais State (Southeast of Brazil), and Peru. The other clade grouped two workers from Rondônia State, west of the Amazonian biome (North of Brazil), specimens bearing considerable variation of pilosity, head, and body shape when compared with the holotype gyne and all the other female specimens collected for *B. scambognathus*, what eventually included specimens from same localities as the males included in the DNA analysis. This scenario suggests the species has a widespread distribution throughout South America, ranging from southeastern Brazil (State of Minas Gerais) to Peru (the 'true' *scambognathus*) with possible cryptic species present in populations of that taxon in the Amazon biome. The variation observed in other *Basiceros* species for those same characters (e.g., in *B. disciger* and *B. militaris*), and the lack of multiple collections for this potential new species, suggests that *B. scambognathus* could probably be multiple cryptic species based on its distribution and morphological variability.

Overall, the reconstructed phylogeny of *Basiceros* presents a noticeable morphological trend within both recovered clades. All analyses recovered the *singularis* clade consisting of *B. manni*, *B. singularis*, *Basiceros* sp. n. A, and *B. convexiceps*. *Basiceros manni* is very similar to *B. singularis* in several characteristics of both the female and male caste, such as size, morphology in general (especially in the head), and pilosity. Moreover, workers of these two

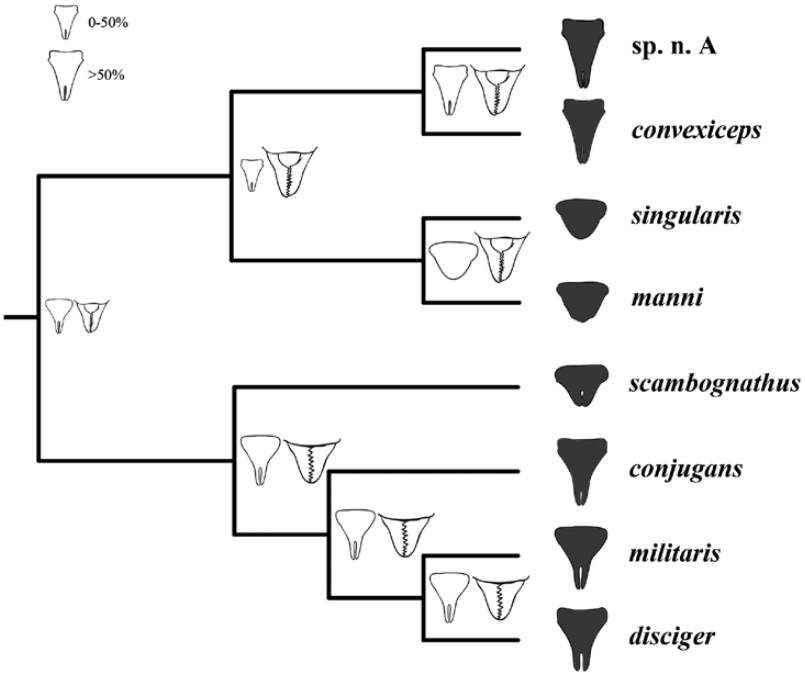

Fig. 6. Ancestral trait estimation for labrum (general shape and distal margin) and clypeomandibular space of *Basiceros* ants. Analyses were conducted with the *ace* function in the APE R package (Paradis et al. 2004) using the pruned1 topology as input (see Material and Methods section). For all traits, each node is graphically represented for the state with the highest probability for the model favored under a likelihood ratio test (see Supp Figs. S2 and S3 and Table S6 [online only]). Graphic size corresponds with likelihood probabilities for a particular node: small graphics represents 0–50% probability, bigger graphics > 50%. Tips present labrum outline for each of the *Basiceros* species (see Fig. 2). Outcomes for each node for the ER model are shown in more detail in Supp Figs. S3 and S4 (online only).

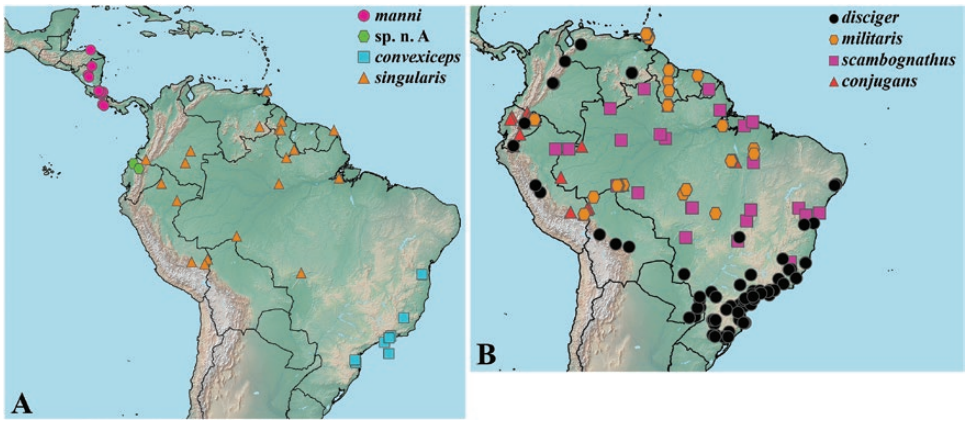

Fig. 7. Distribution map of *Basiceros*. (A) *singularis* clade; (B) *disciger* clade. Georeferenced specimen records from Probst (2015).

species, when covered with litter particles and soil, are hard to tell apart; together with *Basiceros* sp. n. A, workers of those three species share some characteristics such as size, head shape, specialized pilosity on the vertexal margin (long and clavate apically), and the dense specialized hairs on the dorsum of the fourth abdominal segment (=first gastral tergite). Furthermore, there is a strong association between the integumental particles and hair morphology for those species, and workers usually present a dense cover of particles. For the *disciger* clade, consisting of *B. conjugans*, *B. disciger*, *B. militaris*, and *B. scambognathus*, it is noticeable that the particle cover is comparatively scarce, reinforcing the role of the double layer of specialized pilosity for *Basiceros* as a collector for soil and litter fragments, as already pointed out by Hölldobler and Wilson (1986). In general, the specialized pilosity of female ants in this clade is restricted to some parts of the body, and the adherence of particles seems to be facilitated by the foveate-punctuate sculpture present on most of their dorsa. Those species are also considered cryptobiotic; thus, the integumental sculpture appears to have a more critical camouflaging role for that clade.

Mouthpart Evolution

In adult insects, the labrum forms an anterior wall of the mouth cavity on the ventral edge of the face (Snodgrass 1993), primarily functioning in protecting that cavity. Labral shape varies in insects with specialized mouthparts, ants being a great example of variation observed for this trait. Although previous studies have not directly addressed the evolution of the labrum among ants, it has been suggested that a bilobed labrum is a plesiomorphic condition in Myrmicinae (Gotwald 1969). This flap-like sclerite is remarkably diverse within that subfamily, with myrmicine ants expressing it with

a variety of shapes, sizes, sculpture, and pilosity. However, little is known about the functional morphology of such a plastic structure for that subfamily, with most information published restricted to the so-called 'trap-jaw' ants where the labrum was described as playing a pivotal role in prey capture by keeping the mandibles locked in an open position (Brown and Wilson 1959, Masuko 1984, Gronenberg 1996, Gronenberg et al. 1998). Additionally, tactile hairs ('trigger hairs') are present in the distal margin of the labral lobes of those ants, considered to be 'range finders' during foraging, and eventually eliciting mandible action when touching the prey (Gronenberg 1996).

Regarding their plasticity, trap-jaw ants present remarkable variation in mouthparts (Brown and Wilson 1959, Bolton 1999). The tropicopolitan genus *Strumigenys* is an excellent example, with ancestral short mandibulate forms evolving multiple times to long mandibulate forms (D. Booher, University of Illinois at Urbana–Champaign, IL, personal communication). Within *Strumigenys*, the labrum is commonly reduced in size to accommodate mandibular elongation. In *S. zeteki*, although mandibles and trigger hairs are short, labral lobes are long and prominent and presumably help to deal with the antagonistic response of springtails while being subdued (Brown and Wilson 1959). In *S. myllorhapha*, a species with relatively long mandibles, apparently the labral lobes further elongated to accommodate the shortness of the trigger hairs, followed by mandibular elongation (Brown and Wilson 1959).

For the *Basiceros*-genus group, Brown and Kempf (1960) cite the prominent and heavily sclerotized labrum as diagnostic for the group and suggest that the function is to hold prey tightly (Wilson and Brown 1984). Within the group, labrum shape is highly variable, perhaps indicating different levels of feeding specialization. Three genera in the group (*Eurhopalothrix*, *Octostruma*, and *Rhopalothrix*) have received recent taxonomic treatments (Longino 2013a,b; Longino and Boudinot 2013), highlighting the remarkable variation of labral morphology and its importance in species identification (see Fig. 2 in Longino 2013a, Fig. 1 in Longino 2013b, and Fig. 2 in Longino and Boudinot 2013). However, those genera have more species (53, 34, and 16 species, respectively, Bolton 2019) when compared with *Basiceros*, yet even the relatively few species in *Basiceros* exhibit striking labral differences (Fig. 2).

Basiceros has a wide range of variation for the combination of labrum shape and clypeomandibular space (Figs 2–4). Regarding the dorsolabrum, all species have specialized setae along the lateral-anterodorsal margin (see Fig. 2) and share what Bolton (1998) considered to be a synapomorphy for the *Basiceros*-genus group: a deeply incised, transverse groove across the entire basal width, close to the anterior clypeal margin (see Fig. 2C). Some *Basiceros* species have conspicuous anterior lobes on the labrum (Fig. 2A–D), and one interpretation is that the anterior lobes evolved as an anterior projection of the dorsolabrum surface. This reasoning comes from the noticeable uneven surface of the whole sclerite, with the dorsum surface clearly extending over the ventral surface. Interestingly, in species from the *singularis* clade, the lateral and anterior limits of the dorsolabrum are not very discernible from the ventrolabrum, suggesting a flattening (or fusion) of both surfaces during development (see Fig. 3F and G). In contrast, species from the *disciger* clade present a somewhat distinct limit between the dorsolabrum and the ventrolabrum. The ventral view of the whole sclerite shows that the anterodorsal expansion (i.e., the bilobed lobes) is projected forward, with the ventrolabrum underlying it, like a 'basal plate' (see Fig. 3E).

Regarding the ventrolabrum, *Basiceros* labra have conspicuous deflexed sclerotized areas (tormae) on the posterolateral portions, structures associated with the insertion of the posterior frontolabral muscle (=lateral labral retractor; see Fig. 3G). The extensive literature regarding trap-jaw ants and their mandibular mechanisms does not mention any apparent labrum-associated muscle besides the labral adductor muscle (=anterior frontolabral muscle), responsible for latching the trigger movement. Although not investigated here, labral adductor muscles seem to be present in *Basiceros* species (see Fig. 3G), probably contracting to keep the mouthparts protected. It would be interesting to examine whether during hunting (e.g., Fig. 1C) or prey manipulation (see Wilson and Brown 1984), those ants use the anteroventral clypeal margin to hold the labrum in a fixed position. In this way, the labrum would slip forward by the dilation of the lateral labral-retractor muscle, causing contact with the anteroventral clypeal border, thus offering a functional explanation for Bolton's synapomorphy of the deeply incised, transverse groove on the dorsolabrum (Bolton 1998).

Additionally, on the ventral margin, *Basiceros* labra have a cluster of specialized setae along the margin of the 'basal plate' (see Fig. 3F). Although the functional morphology of labral setae is not understood for the group, the presence of specialized ventrolabral pilosity reinforces the scenario in which workers extend the labrum while foraging, using those hairs as proprioceptors or mechanoreceptors. One could speculate that *Basiceros* workers have their heads in parallel to the ground while foraging, either on interstitial leaf litter fauna or on scavenging.

From our analysis, the estimated ancestral state for *Basiceros* mouthparts is a labrum that is long triangular and distally bilobed with a narrow cleft, clypeomandibular space absent (Fig. 6). The latter is associated with a modification of the basal margin of the mandibles, suggesting a link between the basal margin concavity and pedunculate mandibles with the labral morphology (Figs. 2 and 3). In *Basiceros*, it appears that the elongation of mandibles is associated with the appearance of a conspicuous clypeomandibular space, as evidenced by the ancestral state reconstruction for the *singularis* clade, with labral modifications evolving later to fill the clypeomandibular space, to protect the mouth cavity (see Fig. 6). For instance, *B. convexiceps* and *Basiceros* sp. n. A have a conspicuous clypeomandibular space (Fig. 4H and G) and a long triangular and acute labrum (Fig. 2B and H). However, in the latter, the gap between the basal margin of the mandibles and the anterior margin of the clypeus is more significant, and the labrum is reduced, with the lobes almost fused. More evidence for this morphological scenario can be found in the *disciger* clade, with *B. conjugans*, *B. militaris*, and *B. disciger* either lacking or having only a narrow clypeomandibular space (Fig. 4A–C) with the labrum having a conspicuous bilobed distal margin (Fig. 2A, C, and D). The ancestral state reconstruction for the *disciger* clade suggests that in that clade the triangular labrum shape became conspicuously concave, with the anterior cleft between the lobes differentially evolving in the taxa within the clade, but always present.

The clade containing *B. singularis* and *B. manni* shows a striking modification of the labrum (Fig. 2F and G), with both species having a highly specialized, somewhat lunate labrum with a rounded distal margin. Interestingly, in *B. manni* the distal margin has a medially protruding knob, suggesting that although these two species might overlap in their niches, they might prey on slightly different items. It is possible that, in conjunction with a shift from a long triangular to a rounded labrum to fill the space created by the elongated and basally concave mandibles, the shift also evolved as a novel adaptation for feeding preference. Although there is no description of either *B. manni* or *B. singularis* directly using their labrum while foraging, some accounts may explain this unusual behavior in feeding

preferences. Longino (1999) reported from Corcovado National Park, Costa Rica, the presence of nest chambers of *B. manni* with larvae and empty gastropod shells with a long pointed spiral. Additionally, another nest of *B. manni* collected by Ted Schultz (Smithsonian Institution, Washington, DC) at La Selva Biological Station (also Costa Rica), contained abdomens of termites, several unidentified objects, and empty gastropod shells similar to those reported by Longino. Those pointed gastropods shells probably belong to the family Subulinidae [potentially of the genera *Beckianum* Baker or *Allopeas* (Baker), recognized as litter predators (J. Jardim, Museu de Zoologia da Universidade de São Paulo, São Paulo, Brazil, personal communication)]. Nesting material collected in Nicaragua by Michael Branstetter (USDA-ARS Pollinating Insects Research Unit, Logan, UT) also had empty gastropod shells, which appear to belong to a gastropod in the Zonitidae, probably of a *Glyphyalinia* species Martens, 1892 (J. Jardim, personal communication).

Direct evidence of *Basiceros* preying on gastropods comes from photographic accounts. In the exhibition based on photos from Dr. Mark Moffett (Research Associate at the Smithsonian Institution)—'Farmers, Warriors, Builders: The Hidden Life of Ants')—organized at the United States National Museum in 2009, an image depicts a *B. singularis* worker (identified as *B. conjugans*) potentially preying on a pointed and spiral gastropod. Another visual report of this behavior also comes from Mark Moffett in the August 2008 issue of *National Geographic* magazine. One of the photos records the moment when a larva of *B. singularis* feeds on a gastropod with a rounded shell, similar to the one recorded by Branstetter inside *B. manni* nests in Nicaragua. This particular feeding preference reinforces the phylogenetic signal between *B. singularis* and *B. manni*, species with similar mouthpart morphology.

For other *Basiceros* species, data on feeding preference are scarce. Part of a colony of *B. conjugans* was collected in Peru, Madre de Díos nesting in a rotten log, and the trash chamber included a gastropod shell, ant remains, and a cephalic capsule of *Uncitermes teevani* (Isoptera: Syntermitinae) (Probst 2015), suggesting that *B. conjugans* could have scavenger habits. Interestingly, Wilson and Brown (1984) found that *Eurhopalothrix heliscata* also scavenges for termite heads. No information is known about the feeding biology of *B. disciger*, *B. militaris*, and *B. scambognathus*. The natural history of *B. scambognathus* should be of particular interest because of the very distinctive mandibular and labral morphologies (Figs. 2E, 3D, and 6).

Mandible shape is known to be a highly labile trait in ants; however, the labrum is often overlooked in the discussions of mouthpart evolution. This work provides the first step for examining ecological specialization of members of the *Basiceros*-genus group in the light of mouthpart traits, showing transitions in the mandible and labrum, probably due to prey specialization. Moreover, the identification of morphological syndromes might support the investigation of the evolutionary plasticity and lability of ant mouthparts, with the *Basiceros*-genus group being a great model for analysis of that nature. Shared niches could result in similar evolutionary pressures, with well-known cases where worker ant morphology has led to different inferences about true affinities when compared with molecular data (e.g., Moreau et al. 2006, Keller 2011, Ward 2011, Brady et al. 2014, Ward et al. 2015). Therefore, integrating molecular phylogenetics with a careful morphological analysis of mouthparts might help clarify true affinities among ant species.

Conclusion

In closing, this study confirms the monophyly of the *Basiceros* dirt ants at both the genus level and the individual species in the genus. Morphological and molecular data provide support for two distinct clades within the genus. We hypothesize either an origin for the group in the Atlantic Forest of Brazil or the northwestern portion of the Amazon basin, and further exploration might clarify the biogeographic implications for the evolution of the group. Last, our reconstruction for the morphological evolution of mouthparts infers a long triangular and distally bilobed labrum with a narrow cleft and the absence of the clypeomandibular space as the ancestral state for the dirt ants. The transitions observed for those traits suggest a diverse and potentially functionally important mouthpart evolution within the genus.

Supplementary Data

Supplementary data are available at *Insect Systematics and Diversity* online.

Acknowledgments

We thank all curators, institutions, and innumerous colleagues who contributed significantly to this study. We are very grateful to Manuela Ramalho for lab and sequencing assistance. Sérgio Vanin and Rodrigo Feitosa for valuable suggestions and careful reading of an early version of the manuscript. John Longino and Michael Branstetter for all thoughtful suggestions and critical review of all versions of the manuscript. Michael Branstetter for sharing UCE data on multiple ingroup specimens. Júlio Chaul for raising important discussion topics during early versions of this manuscript. Brendon Boudinot for the Blu-tak hint and for assistance with GARLI analyses. Jaime Jardim for the gastropod identifications. We thank Gary Umphrey for sharing an unpublished manuscript on the genus *Basiceros*. For taxonomic catalog resources, we thank Barry Bolton, Stan Blum, Brian Fisher, and the AntCat community; for AntWeb, we thank Brian Fisher. The editor, Marek Borowiec and two anonymous reviewers are thanked for their careful reading of the manuscript and for their constructive comments. R.S.P. acknowledges the support of Coordenação de Aperfeiçoamento de Pessoal de Nível Superior - Brasil (CAPES) - Finance Code 001. The molecular portion of this research was completed in the Pritzker Laboratory for Molecular Systematics and Evolution at the Field Museum of Natural History, Chicago, IL, and supported in part by National Science Foundation (NSF IOS 1916995) to C.S.M. and the Polk Family Charitable Fund (Independent foundation, Bridge Number: 6175270444) to C.S.M. The authors declare no conflict of interest.

References Cited

AntWeb. 2019. (https://www.antweb.org) (Accessed 8 April 2019).

Baroni Urbani, C., and M. L. De Andrade. 2007. The ant tribe Dacetini: limits and constituent genera, with descriptions of new species (Hymenoptera, Formicidae). Ann. Museo Civico Storia Nat. 'Giacomo Doria' 99: 1–191.

Bolton, B. 1998. Monophyly of the dacetonine tribe-group and its component tribes (Hymenoptera: Formicidae). Bull. Nat. History Museum (Entomol. Ser.) 67: 65–78.

Bolton, B. 1999. Ant genera of the tribe Dacetonini (Hymenoptera: Formicidae). J. Nat. Hist. 33: 1639–1689.

Bolton, B. 2003. Synopsis and classification of Formicidae. Mem. Am. Entomol. Inst. 71: 1–370.

Bolton, B. 2019. An online catalog of the ants of the world. (http://antcat.org) (Accessed 9 April 2019).

Brady, S. G., T. R. Schultz, B. L. Fisher, and P. S. Ward. 2006. Evaluating alternative hypotheses for the early evolution and diversification of ants. Proc. Natl. Acad. Sci. USA 13: 18172–18177.

Brady, S. G., B. L. Fisher, T. R. Schultz, and P. S. Ward. 2014. The rise of army ants and their relatives: diversification of the specialized predatory doryline ants. BMC Evol. Biol. 14: 93.

Branstetter, M. G., J. T. Longino, P. S. Ward, and B. C. Faircloth. 2017. Enriching the ant tree of life: enhanced UCE bait set for genome-scale phylogenetics of ants and other Hymenoptera. Methods Ecol. Evol. 8: 768–776.

Brown, W. L., Jr. 1949. Revision of the ant tribe Dacetini: IV. Some genera properly excluded from the Dacetini, with the establishment of the Basicerotini, new tribe. Trans. Am. Entomol. Soc. 75: 83–96.

Brown, W. L., Jr. 1974. A supplement to the revision of the ant genus *Basiceros*. J. N. Y. Entomol. Soc. 82: 131–140.

Brown, W. L., Jr., and W. W. Kempf. 1960. A world revision of the ant tribe Basicerotini. Studia Entomol. 3: 161–250.

Brown, W. L., Jr., and E. O. Wilson. 1959. The evolution of the dacetine ants. Q. Rev. Biol. 34: 278–294.

Darriba, D., G. L. Taboada, R. Doallo, and D. Posada. 2012. jModelTest 2: more models, new heuristics and parallel computing. Nat. Methods 9: 772.

Dietz, B. H. 2004. Uma revisão de Basicerotini Brown, 1949 (Formicidae: Myrmicinae), suas relações filogenéticas internas e com outras tribos dacetíneas (Dacetini e Phalacromyrmecini). Doctoral dissertation, Instituto de Biociências da Universidade de São Paulo (IB/USP), São Paulo, Brazil. 245 pp.

Donisthorpe, H. 1939. Descriptions of several species of ants (Hymenoptera) taken by Dr. O. W. Richards in British Guiana. Proc. R. Entomol. Soc. Lond. B 8: 152–154.

Feitosa, R. M., C. R. F. Brandão, and B. H. Dietz. 2007. *Basiceros scambognathus* (Brown, 1949) n. comb., with the first worker and male descriptions, and a revised generic diagnosis (Hymenoptera: Formicidae: Myrmicinae). Papeis Avulsos Zool. 47: 15–26.

Gotwald, W. H., Jr. 1969. Comparative morphological studies of the ants, with particular reference to the mouthparts (Hymenoptera: Formicidae). Cornell Univ. Agric. Exp. Stat. Mem. 408: 1–150.

Gronenberg, W. 1996. The trap-jaw mechanism in the dacetine ants *Daceton armigerum* and *Strumigenys* sp. J. Exp. Biol. 199: 2021–2033.

Gronenberg, W., C. R. F. Brandão, D. H. Dietz, and S. Just. 1998. Trap-jaws revisited: the mandible mechanism of the ant *Acanthognathus*. Physiol. Entomol. 23: 227–240.

Hölldobler, B., and E. O. Wilson. 1986. Soil-binding pilosity and camouflage in ants of the tribes Basicerotini and Stegomyrmecini. Zoomorphology 106: 12–20.

Hölldobler, B., and E. O. Wilson. 1990. The ants. Belknap Press of the Harvard University Press, Cambridge, MA. 732 pp.

Janda, M., D. Folková, and J. Zrzavy. 2004. Phylogeny of *Lasius* ants based on mitochondrial DNA and morphology, and the evolution of social parasitism in the Lasiini (Hymenoptera: Formicidae). Mol. Phylogenet. Evol. 33: 595–614.

Katoh, K., and D. M. Standley. 2014. MAFFT: iterative refinement and additional methods, vol. 1079. *In* D. Russell (ed.), Multiple sequence alignment methods. Methods in molecular biology (methods and protocols). Humana Press, Totowa, NJ.

Keller, R. A. 2011. A phylogenetic analysis of ant morphology (Hymenoptera: Formicidae) with special reference to the poneromorph subfamilies. Bull. Am. Mus. Nat. Hist. 355: 1–90.

Kumar, S., G. Stecher, and K. Tamura. 2015. MEGA7: Molecular Evolutionary Genetics Analysis version 7.0 for bigger datasets. Mol. Biol. Evol. 33: 1870–1874.

Larabee, F. J., and A. V. Suarez. 2014. The evolution and functional morphology of trap-jaw ants (Hymenoptera: Formicidae). Myrmecol. News 20: 25–36.

Larabee, F. J., B. K. Fisher, C. A. Schmidt, P. Matos-Maraví, M. Janda, and A. V. Suarez. 2016. Molecular phylogenetics and diversification of trap-jaw ants in the genera *Anochetus* and *Odontomachus* (Hymenoptera: Formicidae). Mol. Phylogenet. Evol. 103: 143–154.

Larkin, M. A., G. Blackshields, N. P. Brown, R. Chenna, P. A. McGettigan, H. McWilliam, F. Valentin, I. M. Wallace, A. Wilm, R. Lopez, et al. 2007. Clustal W and Clustal X version 2.0. Bioinformatics 21: 2947–2948.

Longino, J. T. 1999. Ants of Costa Rica. (http://ants.biology.utah.edu/genera/basiceros/species/manni/manni.html) (Accessed 13 April 2019).

Longino, J. T. 2013a. A review of the Central American and Caribbean species of the ant genus *Eurhopalothrix* Brown and Kempf, 1961 (Hymenoptera, Formicidae), with a key to New World species. Zootaxa 3693: 101–151.

Longino, J. T. 2013b. A revision of the ant genus *Octostruma* Forel 1912 (Hymenoptera, Formicidae). Zootaxa 3699: 1–61.

Longino, J. T., and B. E. Boudinot. 2013. New species of Central American *Rhopalothrix* Mayr, 1870 (Hymenoptera, Formicidae). Zootaxa 3616: 301–324.

Masuko, K. 1984. Studies on the predatory biology of oriental dacetine ants (Hymenoptera: Formicidae). I. Some Japanese species of *Strumigenys*, *Pentastruma* and *Epitritus* and a Malaysian *Labidogenys*, with special reference to hunting tactics in short mandibulate forms. Insect. Soc. 31: 429–451.

Miller, M. A., W. Pfeiffer, and T. Schwartz. 2010. Creating the CIPRES Science Gateway for inference of large phylogenetic trees. *In* Proceedings of the Gateway Computing Environments Workshop (GCE), 14 Nov. 2010, New Orleans, LA. pp. 1–8.

Moreau, C. S. 2014. A practical guide to DNA extraction, PCR, and gene-based DNA sequencing in insects. Halteres 5: 32–42.

Moreau, C. S., C. D. Bell, R. Vila, B. Archibald, and N. E. Pierce. 2006. Phylogeny of the ants: diversification in the age of angiosperms. Science 312: 101–104.

Paradis, E., J. Claude, and K. Strimmer. 2004. APE: analyses of phylogenetics and evolution in R language. Bioinformatics 20: 289–290.

Probst, R. S. 2015. Revisão taxonômica e analise filogenética de *Basiceros* Schulz, 1906 (Formicidae, Myrmicinae, Basicerotini). Master thesis, Museu de Zoologia da Universidade de São Paulo (MZSP), São Paulo, Brazil. 263 pp.

Rambaut, A. 2016. FigTree v1.4.3: Tree Figure Drawing Tool. (http://tree.bio.ed.ac.uk/software/figtree).

Rambaut, A., A. J. Drummond, D. Xie, G. Baele, and M. A. Suchard. 2018. Posterior summarisation in Bayesian phylogenetics using Tracer 1.7. Syst. Biol. 67: 901–904. doi:10.1093/sysbio/syy032.

Ronquist, F., M. Teslenko, P. van der Mark, D. L. Ayres, A. Darling, S. Höhna, B. Larget, L. Liu, M. A. Suchard, and J. P. Huelsenbeck. 2012. MrBayes 3.2: efficient Bayesian phylogenetic inference and model choice across a large model space. Syst. Biol. 61: 539–542.

Schulz, W. A. 1906. Spolia hymenopterologica. Junfermannsche Buchhandlung, Paderborn, Germany. 355 pp.

Snodgrass, R. E. 1993. Principles of insect morphology, 93rd ed. Cornell University Press, Ithaca, NY. 667 pp.

Sukumaran, J., and M. T. Holder. 2010. DendroPy: a Python library for phylogenetic computing. Bioinformatics 26: 1569–1571.

Sukumaran, J., and M. T. Holder. 2015. SumTrees: phylogenetic tree summarization. (https://github.com/jeetsukumaran/DendroPy).

Ward, P. S. 2011. Integrating molecular phylogenetic results into ant taxonomy (Hymenoptera: Formicidae). Myrmecol. News 15: 21–29.

Ward, P. S., S. Brady, B. L. Fisher, and T. R. Schultz. 2015. The evolution of Myrmicinae ants: phylogeny and biogeography of a hyperdiverse ant clade (Hymenoptera: Formicidae). Syst. Entomol. 40: 61–81.

Wilson, E. O., and W. L. Brown, Jr. 1985 (1984). Behavior of the cryptobiotic predaceous ant *Eurhopalothrix heliscata*, n. sp. (Hymenoptera: Formicidae: Basicerotini). Insect. Soc. 31: 408–428.

Wilson, E. O., and B. Hölldobler. 1986. Ecology and behavior of the Neotropical cryptobiotic ant *Basiceros manni* (Hymenoptera: Formicidae: Basicerotini). Insect. Soc. 33: 70–84.

Zwickl, D. J. 2006. Genetic algorithm approaches for the phylogenetic analysis of large biological sequence datasets under the maximum likelihood criterion. Ph.D. dissertation, The University of Texas at Austin.